Optimal Design of Passive Devices for Verifying On-wafer Noise Parameter Measurement Systems

Aihua Wu, Xingchang Fu, Chen Liu, Chong Li, *Senior Member, IEEE,*
Yibang Wang, Faguo Liang, and Peng Luan

***Abstract*—We propose the optimal design of passive devices that can be used to verify on-wafer noise parameter measurement systems. The design principles result from obtaining the minimum relative uncertainties of four noise parameters: F_{min}, R_n, $|\Gamma_{opt}|$, and $\angle\Gamma_{opt}$ for a wide range of S-parameters of a passive two-port network. A Monte-Carlo (MC) method has been used for the investigation and the simulation results show that $|S_{11}|$ plays a primary role in deciding the optimal design and must be within 0.5 to 0.6. $|S_{21}|$ plays a secondary role in the design and ideally it should be as small as possible. Based on these findings, we designed and fabricated three planar attenuators on a semi-insulating GaAs substrate. The test results (at up to 40 GHz) show excellent agreement with the simulation. This is the first time that the effect of different designs of passive verification devices on the system noise measurement has been analysed and the design principles of optimal passive devices are given.**

***Index Terms*—Noise parameters, verification devices, mismatch attenuators, relative uncertainty, on-wafer measurement.**

I. Introduction

NOISE is one of the most important parameters for low-noise transistors and amplifiers because the noise figure reflects how much additional noise is added to a signal when passing through such devices. The optimum noise performance of an active device does not necessarily happen at its minimum noise figure, which is normally measured on a 50-Ω test system, but depends on the source impedance. Therefore, the better to describe the noise property of a device three noise parameters (the minimum noise figure, F_{min}, the noise equivalent resistance, R_n, and the optimum reflection coefficient, Γ_{opt} or four noise parameters if Γ_{opt} is written in the format of magnitude $|\Gamma_{opt}|$ and phase $\angle\Gamma_{opt}$) are used as measures of merit [1]. We used four noise parameters throughout this work, unless specified otherwise.

Noise parameter measurements at microwave and millimetre-wave frequencies are challenging due to the low power levels involved and are extremely sensitive to small errors, especially for on-wafer measurements due to greater uncertainties arising from the probes and complications in uncertainty analysis and calculation [2], [3]. Therefore, it is essential to verify the test systems. The method of Simpson *et al*, is based on the traditional noise parameter measurement method: by measuring the noise figure for the source impedance change, they measured F_{min}, R_n, and Γ_{opt} [4]. On the other hand, the work in [5] and [6] measures a noise correlation matrix and computes noise parameters F_{min}, R_n, and Γ_{opt}. The method described here can be used for their verification irrespective of noise parameter measurement method used.

Over the past fifty years, many verification methods have been developed but the majority are based on waveguide or coaxial connectors for packaged devices. Not until the early 1990s on-wafer verification methods were developed. This is mainly due to the success in realising source tuning for the device under test (DUT) and advances in probing technologies [4].

For early verification methods, simple passive devices such as attenuators, couplers, and transmission lines were used [7], [8]. Frazer and Davidson developed a verification procedure using a simple lossy passive network [9], [10]. The verification method takes the advantage of the fact that the noise factor of a lossy circuit is equal to the inverse of the available gain of the network. In addition, the noise parameters of passive devices are easily linked to their S-parameters that can be traced to national standards available at national metrology institutes such as National Institute of Standards and Technologies (NIST). Escotte suggested either a “cold” FET or a Lange coupler as a passive verification device [11]. This is because these devices have similar input and output port matching to that of actual low noise transistors or amplifiers [12], [13].

Manuscript received xx xx, xx; revised xx xx, xx; accepted xx xx, xx. Date of publication xx xx, xx; date of current version xx xx, xx. *(Corresponding author: Chong Li.)*

A. Wu is with the Metrology Centre, Hebei Semiconductor Research Institute, Shijiazhuang, 050051 China (e-mail: aihua.wu@hotmail.com).

X. Fu is with the Division of Electronic Science and Engineering, University of Southeast, Nanjing, 210096 China (e-mail: pasf365@163.com).

C. Liu is with the Metrology Centre, Hebei Semiconductor Research Institute, Shijiazhuang, 050051 China (e-mail: liuchen0209@foxmail.com).

C. Li is with the Division of Electronic and Nanoscale Engineering, School of Engineering, University of Glasgow, Glasgow, G12 8LT UK (e-mail: chong.li@glasgow.ac.uk).

Y. Wang is with the Metrology Centre, Hebei Semiconductor Research Institute, Shijiazhuang, 050051 China (e-mail: wangyibang_hsri@163.com).

F. Liang is with the Metrology Centre, Hebei Semiconductor Research Institute, Shijiazhuang, 050051 China (e-mail: liangdao80@163.com).

P. Luan is with the Metrology Centre, Hebei Semiconductor Research Institute, Shijiazhuang, 050051 China (e-mail: 13673114370@163.com).

Later, Randa proposed the use of mismatched transmission lines with a reflection coefficient greater than 0.3 as verification devices. These mismatched transmission lines can be used to simulate a poorly-matched low noise amplifier (LNA) in a coaxial measurement system and provide a consistency check on the system [14]. For verification of an on-wafer noise parameter measurement system, a mismatched planar attenuator was developed [15]: this can represent the input impedance of a typical microwave transistor, however, it is believed that passive devices alone are insufficient to verify noise parameter measurement systems as they lack an effective excess noise ratio (ENR) [13]. Adamian [12] and Van den Bosch [13] proposed a verification method using active devices whose matching conditions are similar to that of the DUT. Active devices, however, require high stability in the test environment, especially under varying temperature and humidity, which is rarely achieved in inter-laboratory trials. In 2011, Randa developed an improved verification method using passive and active devices in a cascade [14]. Some of the aforementioned issues can be overcome by using a hybrid passive-active verification device, however, the fact that the traceability problem for active devices remains unsolved, even at national metrology institutes, is a hindrance. So far, only passive devices can provide traceability even for hybrid passive and active devices in a cascade and are thus used for system verification.

For the design of a passive verification device, unfortunately there is no detailed guidance on design principles available in the literature. Broadly speaking it is believed that a passive device should meet the following two requirements: 1) the input impedance of the verification device should be close to that of the DUT and 2) the uncertainty of the verification device should be less than that of the measurement systems. Randa suggested the reflection coefficient of the verification device should be greater than 0.3 without any proof thereof [14].

Here we propose design principles for passive verification devices for verifying any on-wafer noise parameter measurement systems [16], [17]. By using the MC method, we investigated the relative uncertainties of all four noise parameters and identified the range of S-parameters that a verification device should have. Based on this finding, we designed three planar attenuators with S-parameters within, and out of, the required range. The experimental results are consistent with the simulated results.

The remainder of this paper is organised as follows: Section II contains details of the relationship between the four noise parameters and S-parameters of passive devices, Section III describes the MC model and simulation procedure for finding the optimal design parameters of the verification device, Section IV analyses the relative uncertainties of the simulated noise parameter variations with the S-parameters, Section V describes the fabrication of three planar verification devices and salient experimental results: the work is summarised in Section VI.

II. Noise Parameters and S-parameters

The relationship between the four noise parameters and the S-parameter of any two-port passive network is widely available in the literature [16]-[19] and will not be repeated here. We only cite key equations for convenience of our discussion in this paper. According to Bosma's noise wave theorem [1], under thermodynamic equilibrium the noise wave correlation matrix, *C*, of a two-port network can be written as

$$C = \begin{bmatrix} c_{11} & c_{12} \\ c_{21} & c_{22} \end{bmatrix} = k_B \begin{pmatrix} X_1 & -X_{12}S_{21}^* \\ -X_{12}^* S_{21} & X_2 \left|S_{21}\right|^2 \end{pmatrix} \tag{1}$$

where k_B represents the Boltzmann constant, S_{ij} is the S-parameter of the two-port network. The asterisk represents the complex conjugate. X_1, X_2, and X_{12} can be linked to the S-parameters via the following equations:

$$X_1 = (1 - \left|S_{11}\right|^2 - \left|S_{12}\right|^2) T_a \tag{2}$$

$$X_2 = \frac{(1 - \left|S_{22}\right|^2 - \left|S_{21}\right|^2)}{\left|S_{21}\right|^2} T_a \tag{3}$$

$$X_{12} = -\frac{(S_{21}^* S_{11} + S_{12} S_{22}^*)}{\left|S_{21}^*\right|} T_a \tag{4}$$

where T_a represents the physical temperature, which is different from the standard noise temperature T_0 *i.e.*, 290 K, and considered as the ambient temperature of the two-port network in most cases.

All four noise parameters can be derived in the more familiar IEEE representation as follows:

$$F_{\min} = \frac{X_2 - \left|\Gamma_{\text{opt}}\right|^2 \left[X_1 + \left|S_{11}\right|^2 X_2 - 2\,\text{Re}(S_{11}{}^* X_{12}) \right]}{T_0 (1 + \left|\Gamma_{\text{opt}}\right|^2)} + 1 \tag{5}$$

$$R_n = \frac{50}{4T_0} \left\{ X_1 + \left|1 + S_{11}\right|^2 X_2 - 2\,\text{Re}\left[\left(1 + S_{11}\right)^* X_{12} \right] \right\} \tag{6}$$

$$\Gamma_{\text{opt}} = \frac{\eta}{2} \left(1 - \sqrt{1 - \frac{4}{\left|\eta\right|^2}} \right) \tag{7}$$

where

$$\eta = \frac{X_2 \left(1 + \left|S_{11}\right|^2\right) + X_1 - 2\,\text{Re}\left[\left(S_{11}\right)^* X_{12} \right]}{(X_2 S_{11} - X_{12})} \tag{8}$$

From (5)-(8), one can see that noise parameters are linked to the S-parameters of the two-port network, where T_0 is the standard noise temperature (290 K in general) [15]. Since S-parameters can be measured using a vector network analyser (VNA), the traceability of a verification device is ensured. This method has been widely used as an alternative to the conventional noise source-based noise parameter measurement method.

III. The Monte-Carlo Simulation

In Section II it is shown that the noise parameters of a passive two-port network can be calculated from its S-parameters. Based on this relationship, Randa analysed Type B uncertainty of coaxial and on-wafer noise parameter measurements using an MC method [20]. In this work we develop a similar MC simulation approach in which the S-parameters of a potential passive device and the relative uncertainties of the four noise parameters are the input and output parameters, respectively.

By investigating possible S-parameters, we find the minimum relative uncertainties of all noise parameters and then use the corresponding S-parameters to design practical verification devices.

A. Description of the MC Model

In the MC simulation, S-parameters for each verification device are the input parameters and are complex. Randa decomposed them into real and imaginary parts and investigated how Type A, Type B errors, and the correlations between the real and imaginary parts affect the overall uncertainty [21]: however, we will use both the magnitude and phase and real and imaginary of the S-parameters here. The S-parameters can be written in the following format using Euler's formula:

$$S_{ij} = a_{ij} + b_{ij}i = M_{ij}\left(\cos\phi_{ij} + i\sin\phi_{ij}\right) \tag{9}$$

where $a_{ij} = M_{ij}\cos\phi_{ij}$ is the real part and $b_{ij} = M_{ij}\sin\phi_{ij}$ is the imaginary part of the S-parameter M_{ij} and ϕ_{ij} (i, j = 1 or 2) are the linear magnitude and phase in degrees. The uncertainties of the real and imaginary parts of the S-parameters are linked to the magnitude and phase and their uncertainties using the uncertainty propagation formula are as follows:

$$\Delta a = \sqrt{\left(\cos\phi\cdot\Delta M\right)^2 + \left(M\sin\phi\cdot\Delta\phi\right)^2} \tag{10}$$

$$\Delta b = \sqrt{\left(\sin\phi\cdot\Delta M\right)^2 + \left(M\cos\phi\cdot\Delta\phi\right)^2} \tag{11}$$

Substituting (9) to (11) into (5) to (8) causes the uncertainty in the S-parameters to propagate to the noise parameters from whence we derive the uncertainties of the noise parameters. The relative uncertainty of a noise parameter, u_r, is defined by:

$$u_r(NP) = \left|\frac{standard\ uncertainty\ (NP)}{estimate\ (NP)}\right| \tag{12}$$

where NP represents any one of the four noise parameters. Please note that the standard uncertainty and estimate in (12) are derived from the S-parameters using the MC method [20]. Thus, we have S-parameters and their uncertainties as the input parameters of our MC simulation and the output parameters are the relative uncertainties of the noise parameters.

B. Determining the Range of the Input Parameters

There are nine input parameters, including four complex S-parameters, and the temperature. We first examine the range of the S-parameters and the distribution of their uncertainties as the input parameters of the MC simulation. The sources of noise parameter uncertainty in any passive device lie in some physical parameters such as: ENR, cable length varying with temperature, S-parameters uncertainty, validity of assumptions, and so on [22]-[24] and are treated as a black box. Here, the interest lies in the range of the S-parameters and the distribution of their uncertainties rather than how the uncertainties are generated.

To reduce the number of input parameters, we deliberately set S_{22} = 0. This assumption is appropriate as S_{22} exerts negligible influence on the noise parameters when less than 0.2 [19]. In addition, we assume S_{21} = S_{12}. This is true for all reciprocal two-port passive devices. Furthermore, we ignore the effect of temperature as it is assumed to be constant in this work. Thus, we only need to evaluate two parameters (S_{11} and S_{21}) and their uncertainty distributions. Since S_{11} and S_{21} are complex we examine their magnitudes and phases individually.

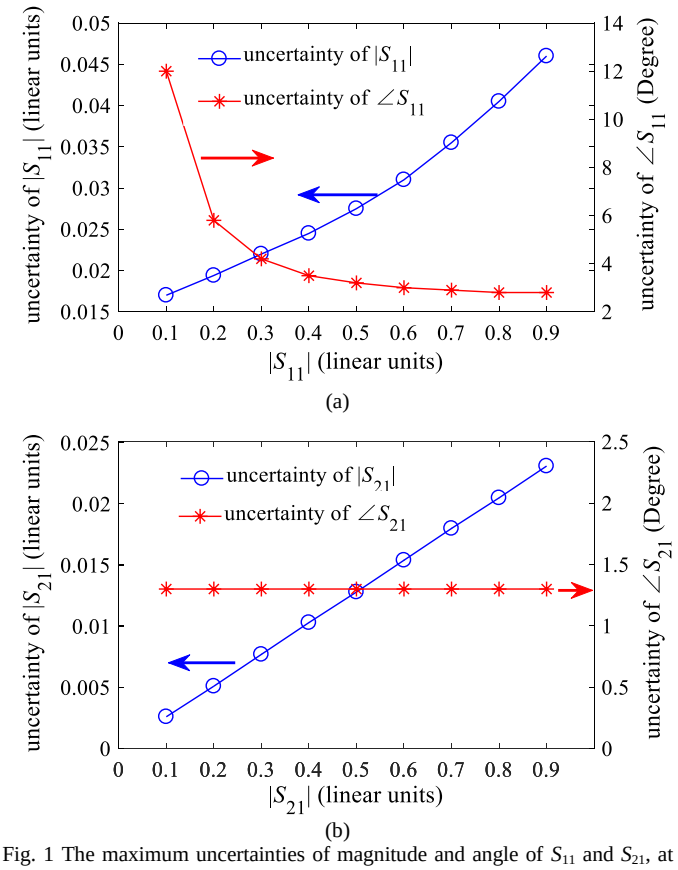

Fig. 1 The maximum uncertainties of magnitude and angle of S_{11} and S_{21}, at frequencies between 1 GHz and 40 GHz, of a coaxial S-parameter measurement system [25]. For convenience we convert the maximum uncertainties of magnitude of S_{11} and S_{21} from decibel to linear measures.

Regarding uncertainty distribution profiles of S_{11} and S_{21}, Randa suggested on-wafer devices have higher uncertainties but similar uncertainty profiles to connectorised devices [19], we then refer to the uncertainty dataset for coaxial cable systems from Keysight [25].

1) S-parameter uncertainties

For convenience we convert the maximum uncertainties from decibel to linear measures and re-plot them (Fig. 1) [26]. From Fig. 1 one can see that the magnitude uncertainties of S_{11} and S_{21} increase monotonically as the magnitudes of S_{11} and S_{21} increase. On the contrary, the phase uncertainties of both S_{11} and S_{21} behave differently. The uncertainty of $\angle S_{11}$ decreases rapidly while $|S_{11}|$ is small and then tends to be stable as $|S_{11}|$ continues increasing (Fig. 1a); however, the uncertainty of $\angle S_{21}$ remains constant for all $|S_{21}|$. This can help us to choose the range of input parameters for our MC simulation. For example, the uncertainties of phase for S_{11} and S_{21} keep constants no matter what their values are once their magnitudes are determined. Therefore, arbitrary phase can be selected and the corresponding uncertainty for phase is adopted according to the determined magnitude to reduce the number of input variables for the simulation.

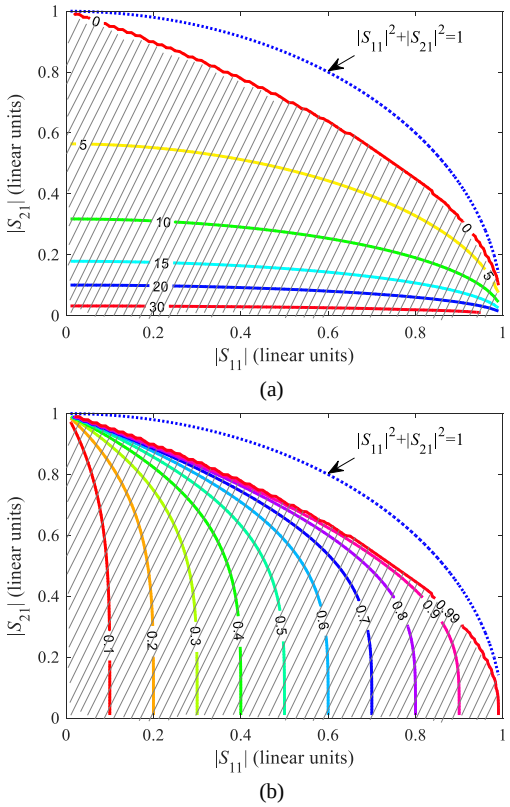

Fig. 2 Possible values of $|S_{11}|$ and $|S_{21}|$ for any passive device as a verification device and the corresponding (a) F_{min} and (b) $|\Gamma_{opt}|$ according to (13)-(15).

2) *Determining the range of* $|S_{11}|$ *and* $|S_{21}|$

The ranges of $|S_{11}|$ and $|S_{21}|$ are limited by the physical and logical constraints of the on-wafer passive two-port network and can be determined by the following equations:

$$|S_{11}|^2 + |S_{21}|^2 \leqslant 1 \tag{13}$$

$$F_{min} > 0 \text{ dB} \tag{14}$$

$$|\Gamma_{opt}| \leqslant 1 \tag{15}$$

We thus plot F_{min} and $|\Gamma_{opt}|$ for various $|S_{11}|$ and $|S_{21}|$ in Fig. 2. The blue dotted curves corresponding to (13) establish upper boundaries of all possible combinations of $|S_{11}|$ and $|S_{21}|$. One can also notice (Fig. 2) that F_{min} (dB) $\approx -S_{21}$ (dB) when $|S_{11}|$ approaches 0 (Fig. 2a) and $|\Gamma_{opt}| \approx |S_{11}|$ when $|S_{21}|$ approaches 0 (Fig. 2a). These two factors are useful when choosing F_{min} and $|\Gamma_{opt}|$.

C. *Probability Distributions of* $|S_{11}|$ *and* $|S_{21}|$

The probability distributions of the input parameters $|S_{11}|$ and $|S_{21}|$ are required for the MC simulation. Since both the real and imaginary parts of the S-parameters have Gaussian distributions [27], we use the standard deviation of the real and imaginary parts of the S-parameters [19], [20].

D. *MC Simulation*

We put probability distribution profiles and possible values of $|S_{11}|$ and $|S_{21}|$ as input variables to the MC model and conduct simulations at a number of frequencies and observe the output relative uncertainties of the noise parameters. The procedure is as follow: fix $|S_{21}|$ to a value starting from 0.1 and conduct the simulation for $|S_{11}|$ from 0.1 to 0.9 with steps of 0.1. Once finished, move to next available value of $|S_{21}|$ with an increment of 0.1 and repeat the simulation for all $|S_{11}|$. This is repeated until all possible $|S_{11}|$ are simulated.

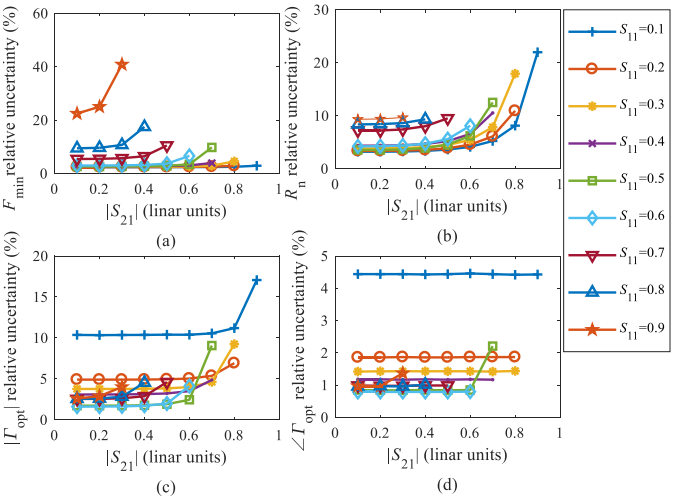

Fig. 3 MC simulated relative uncertainties of noise parameters.

TABLE I
DESIGN PRINCIPLE OF THE PASSIVE VERIFICATION DEVICE

Parameter	Design principle	
	$\|S_{11}\|$	$\|S_{21}\|$
F_{min}	≤ 0.6	≤ 0.9, and the smaller, the better
$\angle\Gamma_{opt}$	[0.5, 0.6]	≤ 0.6, and the smaller, the better
$\|\Gamma_{opt}\|$	[0.5, 0.6]	≤ 0.6, and the smaller, the better
R_n	≤ 0.6	≤ 0.6, and the smaller, the better

IV. SIMULATED RESULTS

Fig. 3 shows the MC simulated relative uncertainties of the four noise parameters. As shown in Fig. 3a, the relative uncertainty of F_{min} increases as $|S_{21}|$ increases for each $|S_{11}|$. In addition, the relative uncertainty also increases as $|S_{11}|$ increases; however, for $|S_{11}| < 0.7$ and a majority of $|S_{21}|$ the relative uncertainty is less than 5%. Based on these observations, we can limit $|S_{11}| \leq 0.6$ and $|S_{21}| \leq 0.9$ for low uncertainty F_{min}. Fig. 3b shows the relative uncertainty of R_n for all possible combinations of $|S_{21}|$ and $|S_{11}|$. One can see similar trends for the relative uncertainty of R_n to that of F_{min}, therefore, we can conclude that, for better performance of R_n, $|S_{11}|$ and $|S_{21}|$ should both be less than 0.6.

Figures 3c and 3d show the relative uncertainties of $|\Gamma_{opt}|$ and $\angle\Gamma_{opt}$. For $|\Gamma_{opt}|$, the relative uncertainty increases as $|S_{21}|$ increases for all $|S_{11}|$ however $0.5 \leq |S_{11}| \leq 0.6$ gives the minimum relative uncertainty. For $\angle\Gamma_{opt}$ although the relative uncertainty remains relatively flat for all $|S_{21}|$ at all $|S_{11}|$, again $0.5 \leq |S_{11}| \leq 0.6$ gives the minimum relative uncertainty.

According to the aforementioned observations we can infer optimal design principles for a passive verification device (Table I). As $|S_{11}|$ has a significant effect on all four noise parameters, and it would be better if it were between 0.5 and 0.6, to achieve the lower relative uncertainties for all four noise

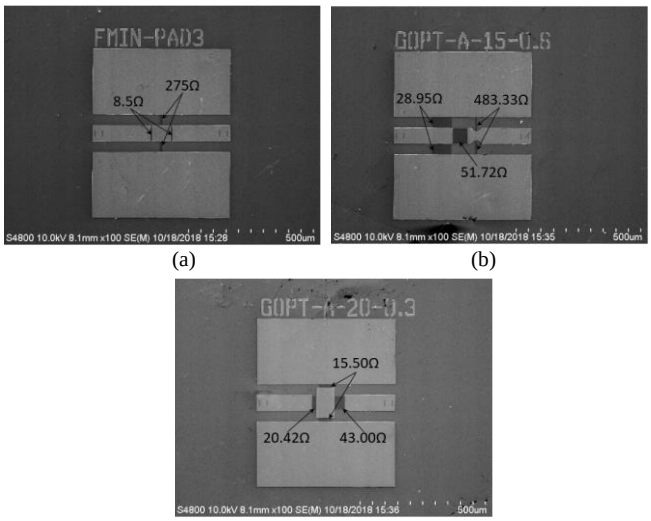

(a) (b) (c)

Fig. 4 Noise parameter verification devices. (a) Matched 3 dB attenuator. (b) Mismatched 15 dB attenuator with a reflection of 0.6. (c) Mismatched 20 dB attenuator with a reflection of 0.3.

parameters. $|S_{21}|$ also influences all noise parameters but should be treated as a secondary consideration, and the smaller, the better.

To verify the simulation results, we have fabricated three attenuators and two of them are outwith the required range and the third one is within optimal design conditions. We will show the design and realisation of the attenuators and discuss the experimental results in the next section.

V. Experimental Results

To verify the design principles, we designed three planar attenuators:

ATTEN1: $|S_{11}| = 0$, $|S_{21}| = 0.71$ (−3 dB), $|S_{22}| = 0$;
ATTEN2: $|S_{11}| = 0.3$, $|S_{21}| = 0.1$ (−20 dB), $|S_{22}| = 0$;
ATTEN3: $|S_{11}| = 0.6$, $|S_{21}| = 0.18$ (−15 dB), $|S_{22}| = 0$.

The verification devices were fabricated on a 500-µm-thick semi-insulating GaAs substrate. The substrate has a nominal dielectric constant of 12.9. 0.5-µm thick gold is used as a conductor and 33-nm thick Nichrome, which gives 50 Ω/square, is used as the resistor film. Photolithography and a standard lift-off process were used to develop the devices. Table II illustrates the nominal properties and tolerances of the materials and fabrication process. A coplanar-waveguide (CPW) line with a nominal characteristic impedance of 50 Ω has the following features: the width of the signal line, the gap between the signal and the grounds, and the width of the grounds are 64 µm, 42 µm, and 300 µm, respectively. Micrographs of the fabricated verification devices are shown in Fig. 4. Along with the verification devices, multiple CPW transmission lines (TMLs) with various lengths including 500 µm, 2685 µm, 3750 µm, 7115 µm, 20,245 µm, and an offset short (275 µm) have also been fabricated on the same substrate. The multiple CPW TMLs are used for system calibration and the calibration method is multiline TRL.

Fig. 5 illustrates the on-wafer S-parameter measurement system which includes a semi-automated probe station from

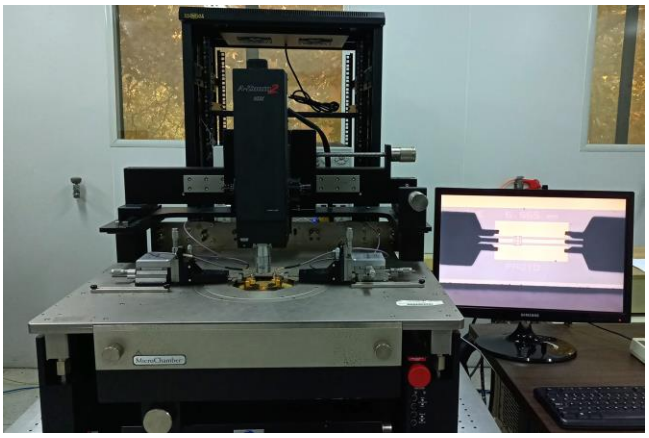

Fig. 5. On-wafer S-parameter measurement system.

TABLE II
Parameters of the Materials and Fabrication Process for Uncertainty Calculation in MUF

Parameter	Nominal Value	Tolerance
Gold geometries	0.5 μm	0.01 μm
GaAs thickness	500 μm	10 μm
Metal conductivity	4.1×10^7 S/m	4.1×10^5 S/m
GaAs dielectric constant	12.9	0.2
Other length	N/A	0.5 μm

Cascade Microtech, Inc., and a 50 GHz Vector network analyser (VNA) from Keysight Technologies. As mentioned previously the multiline TRL calibration method is used for system calibration at 1 GHz, 26.5 GHz, and 40 GHz.

Measurement uncertainties were estimated using Microwave Uncertainty Framework (MUF) from NIST. The framework makes it easy to construct models for calibration standards and automates the calculation of uncertainties with both a conventional linear sensitivity analysis and an MC analysis capable of propagating uncertainties through non-linear models [28]. The MUF is based on propagating changes in physical model parameters through the entire modelling process, and post-processing steps, to the final result. Corrections are included through the entire process, allowing the inclusion of Fourier, and other complex, transforms during data processing. Entities are also provided for including measured errors, and for assessing reproducibility errors from different experiments.

We have implemented the VNA the Uncertainty Calculator from the MUF to calculate measurement uncertainties and uncertainty of the verification devices using the multiline TRL Orthogonal distance-regression algorithm [29]. All major parameters for the calculations are summarised in Table II. We also take into account the ambient temperature which is 296.15 K with an uncertainty of 1 K. Finally, we bring all uncertainties into the MC model described in Section III and plot the results in Figures 6 and 7. From the results:

1) The relative uncertainty of $F_{\min}$ increases slightly with frequency, *i.e.*, by 2.7%, 3.2%, and 4.3% at 1 GHz, 26.5 GHz, and 40 GHz, respectively. In addition, the relative uncertainties of $F_{\min}$ for all three devices are insensitive to changing reflection coefficient.

2) The relative uncertainty of R_n has a similar trend to that of

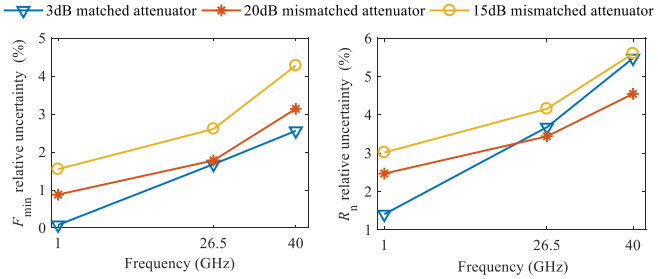

Fig. 6 Relative uncertainties of F_{min} and R_n for three verification devices at 1 GHz, 26.5 GHz, and 40 GHz.

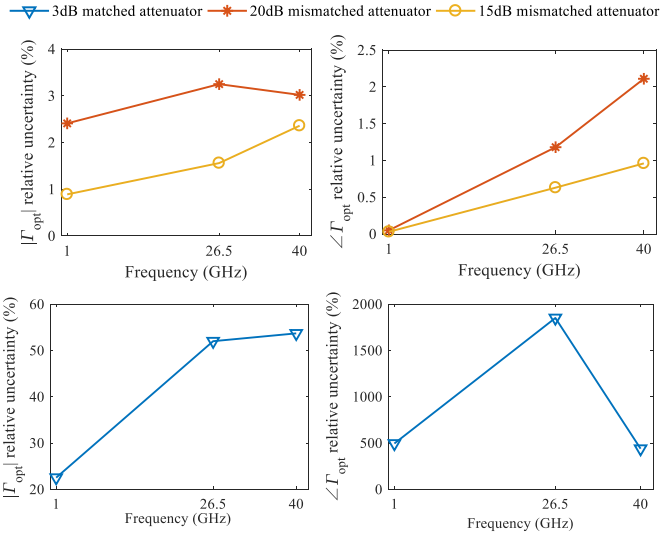

Fig. 7 Relative uncertainties of $\angle\Gamma_{opt}$ and $|\Gamma_{opt}|$ for three verification devices at 1 GHz, 26.5 GHz, and 40 GHz.

F_{min} and the relative uncertainties of all three devices are similar and approximately 5% or less.

3) The relative uncertainties of $\angle\Gamma_{opt}$ and $|\Gamma_{opt}|$ for the devices with a reflection coefficient of 0.3 and 0.6 are less than 3%; however, the matched device has extremely high relative uncertainties for both $\angle\Gamma_{opt}$ and $|\Gamma_{opt}|$.

The experimental results match the simulated results as shown in Fig. 3. In addition, we also measured the three attenuators using a noise parameter measurement system from Maury and Keysight for frequencies between 20 GHz and 42 GHz. The measured noise parameters (solid lines) and the calculated noise parameters (the discrete points) from this work for the three planar attenuators are coplotted in Fig. 8. One can notice that the attenuator with S_{11} equal to 0.6 has close match for all noise parameters but other attenuators do not, especially for $\angle\Gamma_{opt}$. These results also validate our previous conclusion on the optimal design principles for two-port passive verification devices.

VI. Conclusion

We have developed design principles of optimal passive verification device for verifying noise parameter measurement systems using an MC method. By examining the minimum relative uncertainties of all four noise parameters, S-parameters

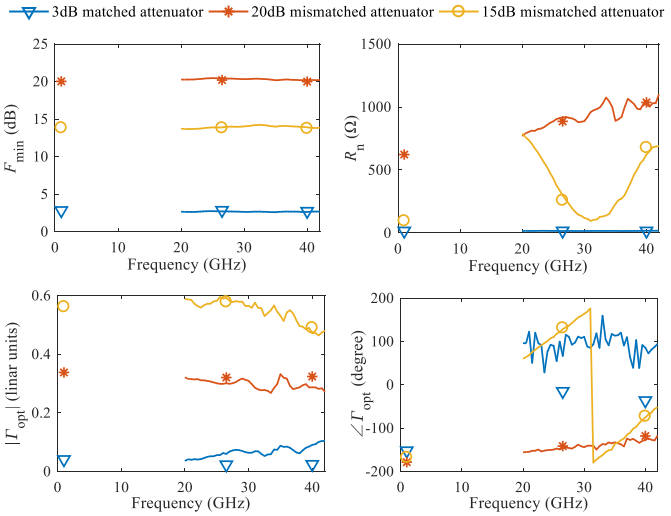

Fig. 8 Comparison of the noise parameters measured using a commercial noise parameter measurement system (solid) and calculated (discrete points) from this work for the three planar attenuators.

of the optimal verification device have been decided. It has been found that $|S_{11}|$ is the primary deciding factor in such a design and has to be between 0.5 and 0.6; $|S_{21}|$ is the secondary factor and should be as small as possible. These design criteria ensure all four noise parameters have less than 5% uncertainty. To prove the design principles, three CPW-based attenuators with different $|S_{11}|$ within, and outwith, the optimum design principle regions were fabricated. The measurement results show excellent agreement with the simulation. This is the first time that the design principals for passive verification devices have been quantified. The design principles can be used for developing both connectorised and on-wafer verification devices. This work has also laid a foundation for more robust composite passive-active verification devices in the future.

Acknowledgment

The authors thank Dr J. Randa and Dr D. Gu of NIST, for their help with this noise parameter uncertainty evaluation.

References

[1] H. Bosma, "On the Theory of Linear Noise Systems," *Philips Res. Repts. Syppl.*, 10, 1967.

[2] J. Randa "Uncertainty analysis for noise-parameter measurements," in *Proc. Conf. Precision Electromagn. Measurements Dig.* Broomfield, CO, USA, 2008, pp. 498-499.

[3] J. Randa, D. K. Walker "On-wafer measurement of transistor noise parameters at NIST," *IEEE Trans. Instrum. Meas.*, vol. 56 no. 2 pp. 551-554, Apr. 2007.

[4] G. Simpson, D. Ballo, J. Dunsmore, A. Ganwani, "A New Noise Parameter Measurement Method Results in More Than 100x Speed Improvement and Enhanced Measurement Accuracy," in *72th ARFTG Microwave Measurement Conference*, Dec. 2008.

[5] D. Pasquet, E. Bourdel, S. Quintanel, T. Ravalet, and P. Houssin, "New method for noise-parameter measurement of a mismatched linear two-port using noise power wave formalism," *IEEE Trans. Microw. Theory Techn.*, vol. 56, no. 9, pp. 2136–2142, Sep. 2008.

[6] A. R. Ahmed, D. H. Lee, and K.W. Yeom, "On-wafer noise parameters measurement using an extended six port network and conventional noise figure analyzer," *Int. J. Microw. Wireless Technol.*, vol. 9, no. 4, pp. 821–829, May 2017.

[7] C. Kim, H. Yu, J. Kim and H. Yoo, "Novel Noise Verification Standard Using a Pi-section RC Network," *Journal of the Korean Physical Society*, Vol. 38, No. 3, March 2001, pp. 215-219.
[8] A. Boudiaf and A. Scavennec, "Experimental investigation of on-wafer noise parameter measurement accuracy," in *Proc. 47th ARFTG Conf. Dig.*, San Francisco, CA, Jun 1996, pp. 20-21.
[9] A. Frazer and E. Strid, "Repeatability and Verification of On-wafer Noise Parameter Measurements," *Microwave J*., pp. 172-176, Nov. 1988.
[10] A. C. Davidson, B. W. Leake, and E. Strid, "Accuracy Improvements in Microwave Noise Parameter Measurement," *IEEE Trans. Microw. Theory Tech.*, vol. 37, no.12, pp.1973-1978, Dec. 1989.
[11] L. Escotte, R. Plana, J. Rayssac, O. Llopis, and J. Graffeuil, "Using cold FET to check accuracy of microwave noise parameter test set," *Electronic Letters*, vol. 27, no. 10, pp. 833-835, May 1991.
[12] V. Adamian and R. Fenton, "Verification of The Noise Parameter Instrumentation," in *Proc. 49th ARFTG Conf. Dig.*, Denver, CO, Jun. 1997, pp.181-190.
[13] S. Van den Bosch, and L. Martens, "Deriving Error Bounds on Measured noise Factors Using Active Device Verification," in *Proc. 54th ARFTG Conf. Dig.*, Atlanta, GA, Dec. 1999, pp. 116–121.
[14] J. Randa, J. Dunsmore, D. Gu, K. Wong, D. K. Walker and R. D. Pollard, "Verification of Noise-parameter Measurements and Uncertainties," *IEEE Trans. Instru. Meas*, vol. 60, no. 11, pp. 3685–3693, Nov. 2011.
[15] K. Kellogg, L. Dunleavy and A.D. Snider, "Temperature Dependent Noise System Verification and the Relationship of Passive Noise Parameters to Available Gain Calculations," in *19th WAMICON Conf. Digest*., Apr. 2018.
[16] A. Wu, C. Li, J. Sun, Y. Wang, C. Liu, "Development of a Verification Technique for On-wafer Noise Figure Measurement Systems," in *90th ARFTG Conf. Digest*., Nov. 2017.
[17] S. Wedge and D. Rutledge, "Noise Waves and Passive Linear Multiports," *IEEE Microw. Guided Wave Lett.*, vol. 1, no. 5, pp. 117–119, May 1991.
[18] S. Wedge and D. Rutledge, "Wave Techniques for Noise Modeling and Measurement," *IEEE Trans. Microw. Theory Tech.*, vol. 40, no. 11, pp. 2004–2012, Nov. 1992.
[19] J. Randa, Uncertainty Analysis for NIST Noise-Parameter Measurements, NIST, Boulder, CO, NIST Tech. Note 1530. [Online]. Available: http://www.nist.gov/eeel/electromagnetics/rf_electronics/noise_publications.cfm
[20] Propagation of distributions using a Monte Carlo method, ISO IEC Guide 98-3 Suppl.1,2008
[21] Uncertainty of Measurement-Part 3: Guide to the Expression of Uncertainty in Measurement, ISO Guide, 2008.
[22] M. Garelli, A. Ferrero, "A unified theory for S-parameter uncertainty evaluation", *IEEE Trans. Microw. Theory Techn.*, vol. 60, no. 12, pp. 3844-3855, Dec. 2012.
[23] M. Wollensack, J. Hoffmann, J. Ruefenacht, M. Zeier, "VNA tools II: S-parameter uncertainty calculation," in *Proc. 79th ARFTG Conf.*, pp. 1-5, Jun. 2012.
[24] G. Avolio, D. F. Williams, S. Streett, M. Frey, D. Schreurs, A. Ferrero, M. Dieudonné, "Software tools for uncertainty evaluation in VNA measurements: A comparative study", in *89th ARFTG Conf.*, pp. 1-7, 2017.
[25] "Keysight 2-Port and 4-Port PNA-X Network Analyzer," Keysight, Santa Rosa, California, USA. Available: https://literature.cdn.keysight.com/litweb/pdf/N5245-90008.pdf?id=1712187
[26] G. Taraldsen, T. Berge, F. Haukland, B. H. Lindqvist and H. Jonasson, "Uncertainty of decibel levels," *J. Acoust. Soc. Am.*, vol. 138, no. 3, pp. 264-269, Sep. 2015.
[27] J. Randa, "Noise-parameter uncertainties: A Monte Carlo simulation," *J. Res. Natl. Stand. Technol.*, vol. 107, pp. 431–444, 2002.
[28] "On-wafer calibration software," National Institute of Standards and Technology, Boulder, Colorado, USA. Available: https://www.nist.gov/services-resources/software/wafer-calibration-software
[29] "NIST Microwave Uncertainty Framework Beta Version," National Institute of Standards and Technology, Boulder, Colorado, USA. Available: https://www.nist.gov/document/nistuncertaintyframeworksetup 01040022exe.

Aihua Wu was born in Zhangjiakou, China, in 1980. He received B.S. and M.E. degrees in Microelectronics from Jilin University (Changchun, China) in 2004 and 2007, respectively.

He joined Hebei Semiconductor Research Institute (Shijiazhuang, China) in 2007. He is a senior research engineer at the Metrology Centre. His research interests include microwave metrology, particularly on-wafer noise measurements and instrumentation, and fabrication of on-wafer devices for ultra-wideband S-parameters and noise parameter calibration and verification. From April to October 2017, he was a visiting researcher at the National Physical Laboratory, UK.

Xichang Fu was born in Laiwu, Shandong, China, in 1975. He received the B.E. in microelectronic technology from Hunan University, Changsha, China, in 1999. He is currently pursuing the Ph.D. degree in Southeast University, Nanjing, Jiangsu, China.

He joined the Hebei Semiconductor Research Institute, Shijiazhuang, in 1999, where he is currently a professor with the Microwave & Millimetre Wave Chip Process Department. His current research interests include microwave semiconductor process, and on-wafer measurement.

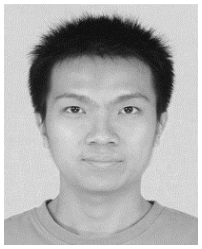

Chen Liu was born in Hengshui, Hebei, China, in 1986. He received B.E. and M.E. degrees in Measuring and Testing Technologies and Instruments from Xidian University (Xi'an, China) in 2009 and 2012, respectively.

He became a Research Engineer in the Metrology Centre at Hebei Semiconductor Research Institute (Shijiazhuang, China) in 2012. His research interests include design and characterization of on-wafer SOLT and TRL *S*-parameters calibration kits, development of accurate on-wafer *S*-parameters and noise parameter measurement techniques, and verification of on-wafer S-parameters and noise parameter using active and passive devices. From April to October 2017, he was a visiting researcher at the National Physical Laboratory, UK.

Chong Li (M'12-SM'17) was born in Liaoning, China in 1979. He received the BEng degree from Donghua University, China, in 2002, the MSc degree (Distinction) from the University of Manchester, UK, in 2007, and the PhD degree in Electronics and Electrical Engineering from the University of Glasgow, UK, in 2011.

He became a Postdoctoral Research Assistant in 2011 and later a Postdoctoral Research Associate at the University of Glasgow, working on development of millimetre-wave signal sources and terahertz imaging systems. He joined the National Physical Laboratory (NPL), UK, in January 2014 as a Higher Research Scientist where he contributed to and led several commercial projects and UK national and European research projects. He was the measurement service provider (MSP) of the ultrafast waveform metrology service at NPL. He also led work on microwave and millimetre-wave on-wafer measurements. He became a lecturer at the University of Glasgow in August 2017 and is currently leading the Microwave and Terahertz Electronics group. His current research interests include microwave and terahertz components, systems and metrology and next generation wireless communications.

Dr. Li is an Associate Editor of *Royal Society Open Science* and has published more than 60 journal and conference papers. Dr. Li held a visiting position at the Advanced Technology Institute (ATI), University of Surrey in 2017 and won the Best Non-student Paper Prize at Loughborough Antennas and Propagation Conference (LAPC) in 2015.

Yibang Wang was born in Jining, Shandong, China, in 1987. He received the B.S. in communication engineering from Nanjing University of Aeronautics and Astronautics, and M.S. degrees in Instrument design in Handan Purified Equipment Research Institute in Hebei, China, in 2012. Then he joined the microwave calibration and test division, Hebei Semiconductor Research Institute in Shijiazhuang, China. His current research interests include microwave metrology, particularly on-wafer Terahertz S-parameters measurements, and the fabrication of on-wafer calibration kits and research of calibration algorithm.

Faguo Liang was born in Liaocheng City, Shangdong Province, China, in 1965. He received B.E. in microelectronics from Shangdong University in 1984, and M.E. in microelectronics from Hebei Semiconductor Research Institute in 1989.

From 1984 to 1986, he was a research assistant with the Jinan Semiconductor Research Institute, China. Since 1989, he was an Engineer with the Hebei Semiconductor Research Institute, China. Now, he is a professor and his research interest include microwave instrumentation metrology, on-wafer microwave parameter measurements.

Peng Luan was born in Liaoning, China, in 1978. He received the B.Eng. degree from North Eastern University, Shenyang, China, in 2002, the M.Sc. degree from University of Electronic Science and Technology of China, Chengdu, China, in 2011, He joined the Metrology Centre, Hebei Semiconductor Research Institute, Shijiazhuang, China, as a Research Engineer in 2002.His current research interests include the design and characterizing of on-wafer TRL S-parameters calibration kits, the development of accurate on-wafer S-parameters and Load-pull system measurement techniques, and the verification of on-wafer S-parameters and Load-pull system using active and passive devices.